Magnetic, magnetoelastic, and electric properties of single-crystal terbium-gadolinium alloys

S. A. Nikitin, N. A. Sheludko, V. P. Posyado, and G. E. Chuprikov

Moscow State University

The concentration dependences of the magnetic, magnetoelastic, and electric properties of single-crystal terbium-gadolinium alloys have been investigated. A restructuring of the Fermi surface has been observed at small gadolinium contents in the alloys. It is shown on the basis of the experimental data on the anisotropy of the paramagnetic Curie points that the magnetic anisotropy in the terbium-gadolinium alloys is due mainly to the single-ion crystal-field mechanism.

PACS numbers: 75.25.+z, 75.30.Gw, 75.50.Cc, 75.80.+q

Indirect exchange interaction and magnetic ordering in heavy rare earth metals (HREM) depend substantially on the energy spectrum of the conduction electrons and on the singularities of the topology of the Fermi surface.[1,2] The influence of the deformation of the Fermi surface on the magnetic properties can be observed by simultaneously investigating the magnetic and electric properties of single-crystal rare-earth alloys. Furthermore, as shown by Irkhin and Karpenko,[3] the study of the magnetic anisotropy of rare-earth alloys in wide range concentrations can explain the nature of the magnetic anisotropy and distinguish between the contributions of the crystal field and the exchange interaction. Thus, data on the magnetic, magnetoelastic, and electric properties are essential if a choice is to be made between the actual physical mechanisms used in modern magnetism theory. However, single crystals of HREM so far have been little investigated.[4-7] Worthy of note are the contradictory conclusions concerning the role played in the magnetic anisotropy of REM and of their alloys by the exchange and single-ion magnetocrystal interactions.[5,8,9]

We have investigated here the magnetic, magnetostriction, and electric properties of the rare-earth terbium-gadolinium alloys, for the purpose of obtaining information that contributes to the solution of the aforementioned problems. Single crystals of alloys of the terbium-gadolinium system were grown by drawing from the melt (by the Czochralski method). An analysis of the impurity concentration has shown that the contents of oxygen, hydrogen, and nitrogen do not exceed 0.01, 0.001, and 0.01 wt.%, respectively, and the combined concentration of the metallic impurities did not exceed 0.01 wt.%. By determining the terbium contents in longitudinal and transverse cuts, we confirmed that the components are uniformly distributed over the length and cross section of the single crystals. The samples used to measure the resistivity were cut with a diamond disk in the three crystallographic directions $\langle 10\bar{1}0 \rangle$, $\langle 11\bar{2}0 \rangle$, $\langle 0001 \rangle$, i.e., along the axes a, b, and c. The magnetization, magnetostriction, and thermal expansion were measured in disks of 0.7–0.9 cm diameter cut in the (ab) and (bc) planes. The samples were etched in a solution of nitric acid in alcohol and annealed in vacuum. The orientation along the indicated crystallographic directions was by the Laue method.

The magnetostriction and the thermal expansion were measured with strain gages having a small galvanomagnetic effect. The magnetic properties were investigated with a vibration magnetometer. The resistivity was determined by a standard four-contact method with a potentiometer circuit.

The resistivity $\rho(T)$ was measured in the temperature interval from 4.2 to 480 K. Above the magnetic-ordering temperature Θ_2, at $T > 400$ K, the resistivity of all alloys increased linearly with temperature both in the basal plane and along the hexagonal axis. The values of $d\rho/dt$ determined experimentally in the paramagnetic state are shown in Fig. 1a. The variation of the topology of the Fermi surface in the course of the alloying of terbium with gadolinium can be traced by using the known relation[10]

$$\frac{d\rho_{\mathrm{ph}}^{i}}{dT} \sim \left(\sum_{s} dS_{i} \right)^{-1}, \tag{1}$$

where i stands for the axes a, b, and c, and $\sum_s dS_i$ is the projection of the Fermi surface on a plane perpendicular to the axis a, b, or c. In the paramagnetic state we have $d\rho_M/dT = 0$,[11] i.e.,

$$\frac{d\rho}{dT} = \frac{d\rho_{\mathrm{ph}}}{dT} + \frac{d\rho_e}{dT}.$$

According to the data of Volkenshtein and co-workers[12] the contribution ρ_e due to electron-electron scattering remains practically unchanged in the case of HREM. As seen from Fig. 1a, $d\rho/dT$ increases weakly along the c axis and decreases along the a and b axes when gadolinium is added to the terbium. It can be concluded on the basis of (1) that addition of gadolinium to terbium decreases somewhat the projection of the Fermi surface on the plane perpendicular to the c axis, and increases its projections on the plane parallel to the hexagonal axis. This seems to correspond to a vanishing of the ribbon singularity of the Fermi surface of terbium,[13] a singularity responsible for the establishment of the antiferromagnetic order of the magnetic moment in terbium.

Definite information on the deformation of the Fermi surface can be obtained also by estimating the deviation of the real Fermi surface S from the area of the Fermi surface of the free electrons $S_{\mathrm{fr\,el}}$ from the relation[14]
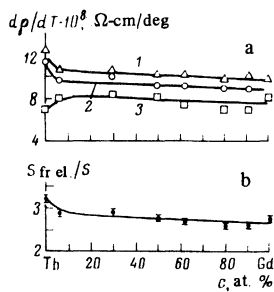
FIG. 1. a) Concentration dependences of dp/dT in the paramagnetic region along the axes b (curve 1), a (curve 2), and c (curve 3). b) Concentration dependence of the ratio $S_{tr\,el}/S$.

$$S_{tr\,el}/S = Z \cdot n^{-1}. \tag{2}$$

Here $S_{tr\,el}$ is the area of a certain hypothetical spherical Fermi surface in the presence of n free electrons per atom, and Z is the Ziman parameter:

$$Z = \frac{4e^2 M k_B \Theta_D^2}{2^{-} \pi^3 h D} \frac{d\rho_{ph}}{dT}, \tag{3}$$

where M is the molecular weight, k_B is Boltzmann's constant, Θ_D is the Debye temperature, and D is the Debye radius.

We have separated ρ_e and $d\rho_e/dT$ by using the results of measurements of the resistivity of single-crystal lutetium by a method described earlier in[12,15]. The value of $d\rho_{ph}^i/dT$ for the crystallographic direction i was determined from the relation

$$\frac{d\rho_{ph}^i}{dT} = \frac{d\rho^i}{dT} - \left(\frac{d\rho_e^i}{dT}\right)_{Lu}. \tag{4}$$

The values of Θ_D and D were obtained for the given alloy by using a linear interpolation from the values for pure metals.[16] Our calculations have shown that for alloys of the Tb-Gd system, in a wide range of concentrations, the Fermi surface is almost independent of composition and changes insignificantly at low gadolinium concentrations (Fig. 1b).

According to our results, at temperatures both below and above the point Θ_2, an appreciable contribution is made to the resistivity by scattering from magnetic inhomogeneities.

Figure 2 shows the determined resistivity component $(\rho_M)_{max}$ due to spin disorder in the paramagnetic state. To separate $\rho_{ph} + \rho_e$ we used the data for single-crystal lutetium, which is an HREM and has no magnetic disorder. The technique of separating ρ_M, ρ_{ph}, and ρ_e was described earlier.[12,15] The magnon contribution to the resistivity, $(\rho_M)_{max}$ increase monotonically in the basal plane with increasing gadolinium concentration, and the anisotropy of $(\rho_M)_{max}$ decreases. At low gadolinium concentrations this contribution is seen to decrease along the c axis.

In the case of binary alloy of the Tb-Gd type, the magnetic contribution to the resistivity in the paramagnetic region can be represented in the form

$$(\rho_M)_{max} = \frac{3\pi (m^*)^2}{4\hbar e^2 k_F v_0} \{x \Gamma_a^2 G_a + (1-x) \Gamma_b^2 G_b - x(1-x) (\Gamma_a S_a - \Gamma_b S_b)^2\}, \tag{5}$$

where the subscripts a and b relate the exchange Γ, the

spin S and the de Gennes factor $G = (g-1)^2 J(J+1)$ to the corresponding components of the alloy $A_x B_{1-x}$; v_0 is the atomic volume, m^* is the effective mass of the conduction electrons, and k_F is the Fermi wave vector.

In analogy with the earlier calculations[4] we have found that $m^* = 2.68 m_e$, $\Gamma = 5.98$ eV $\cdot$ Å^3 for gadolinium and $m^* = 2.82 m_e$, $\Gamma = 5.96$ eV $\cdot$ Å^3 for terbium. Since formula (5) was derived in the isotropic approximation,[11] without allowance for the energy gap in the spectrum of the conduction electrons, it follows that the comparison of the experimental results with the theory is more acceptable for the basal plane. The spins of Tb and Gd differ insignificantly, and the s-f exchange parameters calculated for them are almost equal. For this reason, the third term in (5) does not exceed 2.5% of the total value of the magnetic contribution to the resistivity $\rho_M^\perp$ in the basal plane. The theoretical dependence of $\rho_M^\perp$ on the concentration (dashed in Fig. 2) describes satisfactorily the experimental data.

The expression obtained for the residual resistivity of HREM is[11]

$$\rho^{res} = \rho_{st}^{res} + \rho_M^{res} = \frac{3\pi (m^*)^2 x (1-x)}{4e^2 \hbar k_F^2 v_0} [v_{ab}^2 + (\Gamma_a S_a - \Gamma_b S_b)^2]. \tag{6}$$

Here ρ_{st}^{res} is due to the difference $v_{ab} = v_a - v_b$ of the Coulomb potentials. The residual magnetic resistivity ρ_M^{res} is proportional to $(\Gamma_a S_a - \Gamma_b S_b)^2$. According to the estimate made above, ρ_M^{res} is small in these alloys. The dependence of ρ^{res} on the concentration is close to $x(1-x)$, and the values of ρ^{res} are determined by the contribution ρ_{str}^{res} made by the scattering from the imperfections of the crystal lattice.

The ρ_{str}^{res} level can be estimated from the value of ρ^{res} in Tb and Gd, where $\rho_M^{res} = \rho_{st}^{res} = 0$. In alloys with one magnetic component (e. g., Tb-Y[15]), $\rho_M^{res} \sim (\Gamma_a S_a)^2$ and greatly exceeds the observed values of ρ_M^{res} in Tb-Gd alloys. Thus, for example, at $x = 0.5$ in the system Tb-Y we have $\rho_M^{\perp res} = 32 \times 10^{-6}$ and $\rho_{st}^{\perp res} = 2.5 \times 10^{-6}$ Ω-cm as against $\rho_M^{\perp res} = 0.83 \times 10^{-6}$ and $\rho_{st}^{\perp res} = 0.6 \times 10^{-6}$ Ω-cm for Tb-Gd at $x = 0.5$. The electron shells of the terbium and gadolinium ions are closer in their structure than the electron structure of the yttrium ions. This is reflected in the difference between the values of v_{ab} estimated from the experimental data on ρ^{res} for the systems Tb-Gd and Tb-Y. The difference between the Coulomb potentials of terbium and gadolinium is $v_{Tb-Gd} = 2.69$ eV $\cdot$ Å^3 as against the much larger $v_{Tb-Y} = 5.23$ eV $\cdot$ Å^3. These facts indicate that the theory developed by Dek-
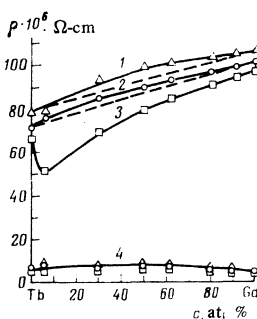

FIG. 2. Concentration dependences of the magnon components of the resistivity $(\rho_M)_{max}$ in the paramagnetic region for the axes b (curve 1), a (curve 2) and c (curve 3) and of the residual resistivity (curve 4).
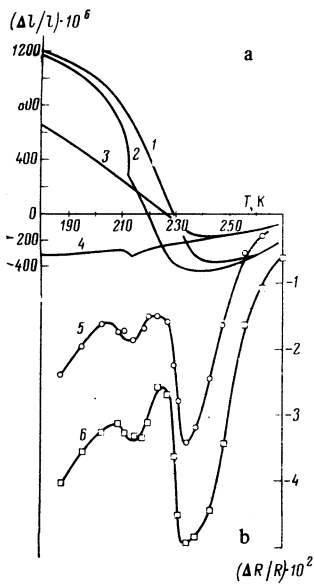
FIG. 3. Relative elongation of the alloy Tb + 6 at.% Gd in thermal expansion: Curves 1—$H \parallel g \parallel b$, $H = 10$ kOe; 2—$g \parallel c$, $H = 0$, 3—$H \parallel b$, $g \parallel c$, $H = 10$ kOe; 4—$g \parallel b$, $H = 0$ (g is the measurement direction). b) Longitudinal galvanomagnetic effect along the easy-magnetization in the crystal Tb + 6 at.% Gd: curves 5—$H = 7$ kOe, 6—$H = 11$ kOe.
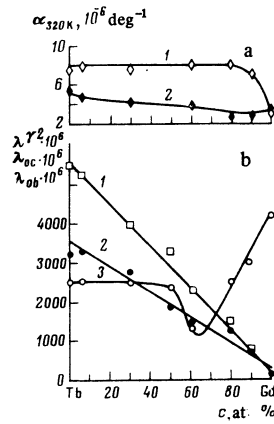

FIG. 4. Magnetoelastic properties of alloys of the Tb-Gd system: a) coefficient of thermal expansion along the hexagonal axis (curve 1) and in the basal plane (curve 2); b) magnetostriction constant $\lambda^{\gamma 2}$ (line 1); spontaneous striction along the b axis, λ_{0b} (line 2); spontaneous striction λ_{0c} along the c axis (curve 3); temperature 4.2 K.

ker[11] describes satisfactorily the singularities of ρ^{res} in HREM alloys.

The results of the investigation of the magnetostriction properties and of the thermal expansion are shown in Figs. 3 and 4. In the region of the magnetic-ordering temperatures there are superimposed on the phonon part of the thermal expansion strong spontaneous magnetostriction deformations whose values in the single-domain state can be obtained from the plots of $\Delta l/l$ against T when an external magnetic field H is applied and destroys the domain structure. The presence of a strong lengthening along the hexagonal axis at 212 K and of a minimum on the plot of $\Delta l/l$ against T near 212 K at $H = 0$ (Fig. 3, curve 4) indicate that in Tb + 6 at.% Gd, just as in Tb, a transition from the antiferromagnetic to the ferromagnetic state takes place at Θ_1. In addition, the presence of two temperatures, Θ_1 and Θ_2, in the Tb + 6 at.% Gd alloy is confirmed by the anomalous temperature dependence of the galvanomagnetic effect: two minima are observed on the $\Delta R(H)/R$ curve, and in weak fields the temperature of the low-temperature minimum of $\Delta R(H)/R$ coincides with the temperature of the sharp change of the crystal-lattice parameters on the relative-elongation curve, Fig. 3. In alloys with 30 at.% Gd and more, no anomalies connected with the first-order transition are observed at the point Θ_1 on the $\Delta R(H)/R$ and $\Delta l(T)/l$ curves.

Calculations of the band structure by the augmented-plane wave method give grounds for assuming that the Fermi surfaces for Tb and Gd are quite close in their structure.[13] The Fermi surface of Tb, however, differs significantly in that it has a "ribbon singularity" on the boundary of the third and fourth zones, and this singularity contributes to the appearance of antiferromagnetic ordering. The absence of this Fermi-surface element in the case of gadolinium causes them not to have a canted magnetic structure. When Tb is alloyed with Gd, antiferromagnetic ordering is observed only at a gadolinium content less than 6 at.%. It is precisely at these concentrations that a certain change takes place in the

structure of the Fermi surface, as indicated by the data on the electric properties (Fig. 1). It appears that the vanishing of the ribbon singularity in the alloys of the Tb-Gd system takes place at a Gd concentration exceeding 6 at.%. The size of the entire Fermi surface, characterized by the ratio $S_{fr\,el}/S$, likewise changes somewhat near 6 at.% Gd (Fig. 1b).

The spontaneous magnetostriction deformations λ_{0c} along the c axis and λ_{0b} along the b axis were determined by us by subtracting the phonon part of the thermal expansion $(\Delta l/l)_{ph}$ from the experimental $(\Delta l/l)^{\parallel}$ and $(\Delta l/l)^{\perp}$ curves measured in a magnetic field applied along the easy-magnetization axis. The value of $(\Delta l/l)_{ph}$ for each alloy was obtained from the thermal-expansion curves of lutetium, which has no magnetic component of the thermal expansion, with incorrection introduced for the difference between the Debye temperatures.[7] λ_{0b} and λ_{0c} have different concentration dependences: λ_{0b} decreases monotonically when Tb is fused with Gd, whereas λ_{0c} has a minimum in the concentration region 60–70 at.% Gd, and with further increase of the gadolinium content λ_{0c} increases rapidly (Fig. 4). The magnetostriction constant $\lambda^{\gamma 2}$, equal to the difference between the longitudinal and transverse magnetostrictions in the basal plane, decreases linearly with increasing gadolinium concentration.

The values of the thermal-expansion coefficients at 320 K change very little in a wide range of concentrations (Fig. 4a). The decrease of $\alpha^{\perp}$ and $\alpha^{\parallel}$ for alloys with large Gd contents is apparently due to the magnetic
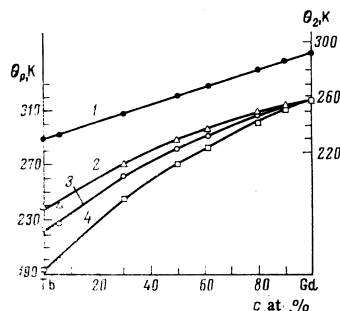
FIG. 5. Critical temperatures of magnetic ordering Θ_2 (1) and paramagnetic Curie points $\Theta_p^{\perp}$ (2), Θ_p^{poly} (3), $\Theta_p^{\parallel}$ (4) for alloys of the Tb-Gd system.
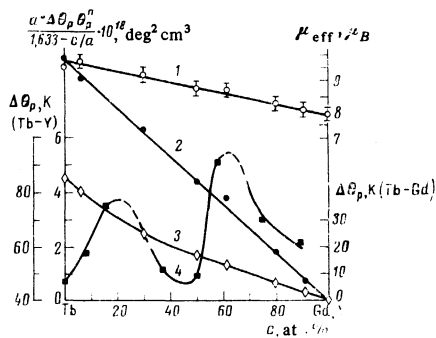
FIG. 6. Effective magnetic moment μ_{eff} (1) and magnetic anisotropy of alloys of the system Tb-Gd: curve 2—plot of $a^3\Delta\Theta_p\Theta_p^{poly}/(1.633-c/a)$, 3—anisotropy of the paramagnetic Curie points; 4—anisotropy of the paramagnetic Curie points in alloys of the Tb-Y system.

contribution to $\Delta l/l$ at 320 K (the Curie points of these alloys are close to each other at room temperature).

The influence of the short-range magnetic order manifests itself also in the deviation from the Curie-Weiss law for the paramagnetic susceptibility at temperatures 50–70° higher than Θ_2. At higher temperature, the reciprocal paramagnetic susceptibility $\chi^{-1}(T)$, measured up to 550 K, varies in accord with the Curie-Weiss Law. From the slopes of the experimental $\chi^{-1}(T)$ curves we determined the effective magnetic moments per atom. μ_{eff} decreases linearly with increasing gadolinium content in the alloy, with $\mu_{eff} = 7.9\,\mu_B$ for Gd and $\mu_{eff} = 9.6\,\mu_B$ for Tb.

By extrapolating the linear section of the $\chi^{-1}(T)$ curves to zero we determined the paramagnetic Curie points $\Theta_p^{\perp}$ (magnetization in the basal plane) and $\Theta_p^{\parallel}$ (magnetization along the hexagonal axis). With increasing gadolinium content, $\Theta_p^{\perp}$ and $\Theta_p^{\parallel}$ increase monotonically, while the difference $\Delta\Theta_p = \Theta_p^{\perp} - \Theta_p^{\parallel}$ decreases (Figs. 5 and 6). The anisotropy $\Delta\Theta_p$ of the paramagnetic Curie points varies nonlinearly with the concentration. The paramagnetic Curie point Θ_p^{poly}, calculated for a polycrystalline sample from the formula $\Theta_p^{poly} = \frac{1}{3}(2\Theta_p^{\perp} + \Theta_p^{\parallel})$ has a nonlinear dependence on the alloy composition (Fig. 5), in contrast to the temperature Θ_2 of the magnetic ordering.

In HREM alloys, the uniaxial magnetic anisotropy constant can be expressed in terms of $\Delta\Theta_p\Theta_p^{poly}$ with allowance for the deviation of the hexagonal crystal lattice from the ideal hexagonal close packed lattice:[5,17]

$$K_2^0 \sim a^3\Delta\Theta_p\Theta_p^{n}/(1.633-c/a). \tag{7}$$

We estimated the effect exerted on K_2^0 by the temperature dependences of the parameters a and c by starting from the obtained experimental data on the thermal expansion of the Tb-Gd alloys. It follows from the calculations that this effect can be neglected. The dependence of $\Delta\Theta_p\Delta\Theta_p^{poly}$ on the concentration, with allowance for the change of the lattice parameters in the investigated alloys [Eq. (7)] is shown in Fig. 6. Since K_2^0 decreases linearly with increasing gadolinium content in the alloys, this allows us to conclude that in the Tb-Gd system the magnetic anisotropy is due mainly to single-

ion magnetocrystal interaction. In the magnetostriction due to the rotation of the magnetization in the basal plane (the constant $\lambda^{\gamma 2}$ in Fig. 4), the single-ion contribution also predominates, as indicated by the linear dependence on the composition. The results agree with the conclusions of an earlier investigation[18] of the temperature dependence of $\lambda^{\gamma 2}$, where it is shown that $\lambda^{\gamma 2}(T)$ for the alloy Tb + 50 at.% Gd is adequately described by the formulas of the single-ion theory.

Some deformation of the Fermi surface takes place in Tb-Gd alloys, according to our calculations, at low gadolinium concentrations. This realignment of the electronic structure is negligible and does not affect the concentration dependence of the paramagnetic Curie points, the magnetic anisotropy, and the magnetostriction constants. The electric properties turn out in this case to be more sensitive. To the contrary, when terbium is alloyed with yttrium, a substantial restructuring of the Fermi surface is observed,[15] and manifests itself in a jumplike change of the temperature coefficients of the resistivity in the paramagnetic region near 40–50 at.% yttrium, and in a deviation of the anisotropy of the paramagnetic Curie points $\Delta\Theta_p$ from the concentration dependence expected for the single-ion theory (Fig. 6). In Tb-Y alloys containing only one magnetoactive rare-earth atom—the terbium atom (the magnetic moment of yttrium is zero), $\Delta\Theta_p$ is a constant according to this theory. The results discussed can be attributed to the fact that in the case when a strong change takes place in the topology of the Fermi surface, a change occurs in the contribution made to the magnetic anisotropy on account of the anisotropic exchange connected with the pair interaction.[3]

In conclusion, we thank Professor K. P. Belov for valuable remarks made in the course of the discussion of the results.

[1]S. V. Vonsovskiĭ, Magnetizm (Magnetism), Nauka, 1971.

[2]I. E. Dzyaloshinskiĭ, Zh. Eksp. Teor. Fiz. 47, 336 (1964) [Sov. Phys. JETP 20, 223 (1965)].

[3]V. P. Karpenko and Yu. P. Irkhin, Zh. Eksp. Teor. Fiz. 64, 756 (1973) [Sov. Phys. JETP 37, 1495 (1973)].

[4]S. A. Nikitin, S. S. Slobodchikov, and O. D. Chistyakov, Zh. Eksp. Teor. Fiz. 70, 104 (1976) [Sov. Phys. JETP 43, 54 (1976)].

[5]R. Z. Levitin, T. M. Perikalina, L. P. Shlyakhina, O. D. Chistyakov, and V. L. Yakovenko, Zh. Eksp. Teor. Fiz. 63, 1401 (1972) [Sov. Phys. JETP 36, 742 (1973)].

[6]A. Mishima, H. Tujii, and T. Okamoto, J. Phys. Soc. Jpn. 39, 873 (1975).

[7]S. A. Nikitin, D. Kim, and O. D. Chistyakov, Zh. Eksp. Teor. Fiz. 71, 1610 (1976) [Sov. Phys. JETP 44, 843 (1976)].

[8]P. Boutron, Phys. Rev. B 9, 2971 (1974).

[9]L. W. Roeland, G. J. Cock, and P. A. Lindgrad, J. Phys. C 8, 3427 (1975).

[10]S. Legvold, Magnetic Properties of R. E. M., Plenum Press, New York, 1972, p. 335.

[11]A. J. Dekker, J. Appl. Phys. 36, 906 (1965).

[12]N. V. Volkenstein, V. P. Dyakina, and V. E. Startsev, Phys. Status Solidi 9, 57 (1973).

[13]M. I. Darby and K. N. Taylor, Physics of Rare-Earth Solids, Chapman & Hall.

[14]J. M. Ziman, Electrons and Phonons, Oxford, 1960.
[15]K. P. Belov, S. A. Nikitin, V. P. Posyado, and G. E. Chuprikov, Zh. Eksp. Teor. Fiz. **71**, 2204 (1976) [Sov. Phys. JETP **44**, 1162 (1976)].
[16]K. A. Gschneider, Rare-Earth Alloys, Van Nostrand, 1961.
[17]T. Kasuya, Magnetism, by G. Rado, G. Suhl, New York,

2B, 1966, p. 216.
[18]S. A. Nikitin, G. E. Chuprikov, K. I. Epifanov, D. Kim, L. A. Voskresenskaya, and M. L. Grachev, Nauchnye trudy Giredmeta **67**, 77 (1976).

Translated by J. G. Adashko

Interactions between electrons and a strong piezoacoustic wave

V. V. Popov and A. V. Chaplik

Institute of Semiconductor Physics, Siberian Division, USSR Academy of Sciences
(Submitted March 4, 1977)
Zh. Eksp. Teor. Fiz. **73**, 1009–1015 (September 1977)

The behavior of electrons trapped by the field of a strong piezoacoustic wave in nondegenerate semiconductors is studied. The resonant absorption of microwaves due to the quantization of one of the electron momentum components in the wave field and the effect of intense ultrasound on the galvanomagnetic properties of the crystal are considered.

An ultrasonic wave (USW) of sufficiently high frequency and intensity can materially change the character of the motion of electrons in a crystal. A number of specific effects arise here, dependent in a nonlinear way on the intensity of the USW. Some of these effects have been investigated in a number of researches.[1-4] In particular, a quantum effect was considered in Ref. 1 and consists of the change in the energy spectrum of the electrons in the field of a strong hypersonic wave ($\nu > 10^9$ Hz); the effect of spatial redistribution of electrons in the field of a USW on sound propagation was studied in Refs. 2–4.

In the present paper, we study the behavior of electrons trapped by the field of a strong piezoacoustic wave in nondegenerate semiconductors. The resonant absorption of microwaves, connected with the quantization of one of the components of the momentum of the electron in the field of the wave, and the effect of a strong ultrasonic signal on the galvanomagnetic characteristics of the crystal, are investigated.

I. RESONANT ABSORPTION OF MICROWAVES

1. *Formulation of the problem. The energy spectrum of the electrons.* Consider the interaction of free electrons with a powerful ultrasonic wave in a nondegenerate piezo-semiconductor (n-type) with isotropic and quadratic dispersion law $E = p^2/2m^*$. In the effective-mass approximation, the action of the wave on the electron reduces to the classical non-stationary potential field

$$V(y, t) = V_0 \cos(ky - \omega t), \quad \omega = sk, \qquad (1)$$

where s is the sound velocity (in the case of a cubic crystal, we deal with transverse sound), V_0 is expressed as a known function of the piezomoduli, of the dielectric tensor, and of the displacement vector in the USW. We

shall be interested in the condition in which $V_0 \gg T$ (the temperature is in energy units). At a displacement amplitude $u_0 = 10^{-9}$ cm, wave frequency $\omega = 2\pi \cdot 10^9$ sec^{-1}, $V_0 = 176$ K for GaAs and $V_0 = 62$ K for InSb, the required power flux is 3.5 W/cm^2 and 1.7 W/cm^2, respectively.

After the carriers reach equilibrium with the wave, they will execute finite motion in y in small (by virtue of the condition $T \ll V_0$) vicinities of the minima of the potential (1). In a system of coordinates moving with the USW, such a motion corresponds to stationary states with quantum energy levels very close to the levels of the harmonic oscillator $E_n = \hbar\Omega(n + \frac{1}{2})$, $n = 0, 1, 2, \ldots$, where $\Omega = (V_0 k^2/m^*)^{1/2}$. The total energy of the electron is equal to $E_n + (p_x^2 + p_z^2)/2m^*$, and its spectrum is, of course, continuous. The effects of anharmonism are connected with the deviation of the actual potential $V_0 \cos ky$ from parabolic and become significant only at large numbers n. However, these levels are practically unpopulated at $T \ll V_0$. For the values of ω and u_0 used above, we obtain Ω (GaAs) $\approx 3.77 \times 10^{11}$ sec^{-1} ($\hbar\Omega \approx 3$ K) and Ω (InSb) $\approx 7.54 \times 10^{11}$ sec^{-1} ($\hbar\Omega \approx 6$ K).[1)] Strictly speaking, each of the found levels is spread out into a band because of the periodicity of the potential (1). However, it is easy to prove that the tunnel transparency of the barriers in the considered case is entirely negligible, i. e., the conditions of applicability of the strong-coupling approximation are satisfied by a wide margin, and we can neglect the widths of the bands.

The condition of good resolution of the discrete levels imposes a restriction on the momentum relaxation time τ of the electrons. That is, the inequality $\Omega\tau > 1$, or $kL(V_0/T)^{1/2} > 1$ must be satisfied, where L is the free path length of the electron. Finding τ from the expression for the mobility, we obtain the conditions μ (GaAs) $> 7.2 \times 10^4$ cm^2/V-sec, μ (InSb) $> 1.7 \times 10^5$ cm^2/V-sec.